Physica C: Superconductivity and its applications 560 (2019) 26–30

Contents lists available at ScienceDirect

Physica C: Superconductivity and its applications

journal homepage: www.elsevier.com/locate/physc

# Epitaxial growth of gradient $Ce_{1-x}Zr_xO_2$ buffer layer for $YBa_2Cu_3O_{7-\delta}$ coated conductors

Li Limin[a], Zhao Gaoyang[a,b], Lei Li[b,*], Yan Fuxue[b], Jia Jiqiang[b], Liu Xiaoqin[a], He Yang[a]

[a] School of Material Science and Engineering, Xi'an University of Technology, Xi'an, Shaanxi 710048, People's Republic of China
[b] Advanced Material Analysis and Test Center, Xi'an University of Technology, Xi'an, Shaanxi 710048, People's Republic of China

ARTICLE INFO

*Keywords:*
Epitaxial growth
Gradient buffer layer
$Ce_{1-x}Zr_xO_2$
Coated conductors

ABSTRACT

A $Ce_{1-x}Zr_xO_2$ (CZO) buffer layer architecture with gradient change of Zr-doped concentration along the thickness direction of CZO films was fabricated on rolling assisted biaxially textured NiW metallic substrate by sol–gel method. With the change of Zr-doped concentration, the lattice parameters of CZO of each layer also show a gradient variation. It can not only effectively reduce interfacial stress between the buffer layer and the metallic substrate, but also improve the surface quality of the CZO film. In this work, an epitaxial growth relationship and dense microstructure are discerned in the gradient CZO film, as determined by the comprehensive analysis of X-ray diffraction and scanning electron microscopy. YBCO superconductor films have been deposited on the gradient CZO buffer layers to evaluate the quality of such a gradient buffer layer. TEM measurements reveal that NiW/CZO/YBCO coated conductor (CC) with excellent epitaxial growth relationship is achieved. The superconducting transition temperature of the sample is 90 K and the critical current density $J_c$ reaches 1.9 MA/cm$^2$.

## 1. Introduction

It is quite necessary to insert a buffer structure between metallic substrate and superconducting film. The buffer layer can serve as a barrier to prevent the diffusion of metal ions between the adjacent layers, and also as a texture transfer template to promote the epitaxial growth of the subsequent superconducting layers [1,2]. Up to now, there have been several kinds of high-performance buffer layer architectures obtained by combinations of multiple deposition processes including $CeO_2$/YSZ/$CeO_2$, $CeO_2$/$La_2Zr_2O_7$, $SrTiO_3$/$Ba_{0.2}Ca_{0.8}TiO_3$ and CZO/YSZ [3–7]. Nevertheless, there are still some drawbacks needed to overcome such as complex preparation route or rather expensive vacuum equipment which leads to the high cost of coated conductors. Therefore, simplifying the buffer layer structure and reducing the manufacturing cost are the essential issues for facilitating the practical development of CC tapes.

$CeO_2$ with the fluorite structure is an ideal candidate to be used as a simplified single buffer layer due to its good chemical stability and compatibility, together with the smallest crystal lattice mismatch and closest thermal expansion coefficient to YBCO [8–10]. Unfortunately, cracks will be generated in $CeO_2$ film when its thickness exceeds ~50 nm, and besides there is a large lattice mismatch with the NiW substrate [11]. Thus several kinds of $CeO_2$ buffer layers doped with smaller ionic radius element have been developed [12–15], which improved the lattice mismatch between $CeO_2$ and NiW substrate. However, it is obviously learned that the lattice mismatch between $CeO_2$ and YBCO superconducting layer will increase, which results in the worse biaxial texture and superconducting properties of YBCO film deposited on the doped $CeO_2$ buffer layer. In order to solve the above problems, a gradient doping strategy is proposed in this work, where zirconium with smaller atomic size ($Zr^{4+}$ = 0.84 Å) is adopted to substitute cerium in the ceria lattice ($Ce^{4+}$ = 0.97 Å) [16] to form gradient CZO buffer architecture which has multilayer Zr-doped $CeO_2$ films with different doping percentage in each layer. One layer with a larger Zr-doping concentration serves as the bottom buffer layer close to the NiW substrate because of the diminished lattice constant, while the other layer with a lower Zr-doping concentration acts as the top buffer layer close to YBCO superconducting layer by reason of the increased lattice constant. Thus, the doping concentration of zirconium element exhibits a gradient change along the thickness direction of the CZO film. Therefore, it is favorable to reduce the lattice mismatch of NiW substrate/buffer layer and buffer layer/YBCO simultaneously, which can increase the film thickness and improve the growth texture of the buffer layer.

* Corresponding author.
*E-mail addresses:* zhaogy@xaut.edu.cn (G. Zhao), leili@xaut.edu.cn (L. Lei).

https://doi.org/10.1016/j.physc.2019.02.002
Received 16 January 2019; Accepted 4 February 2019
Available online 05 February 2019

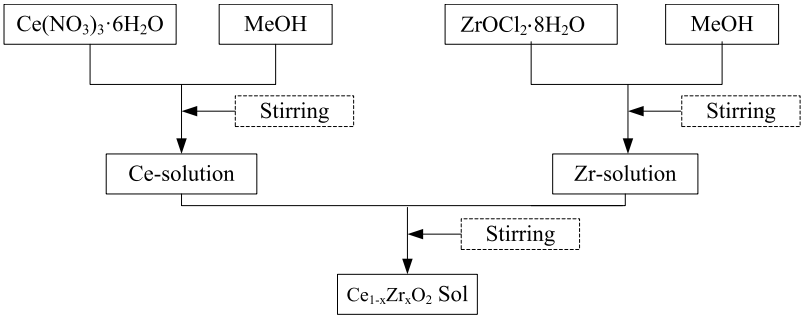


**Fig. 1.** Flowchart for the preparation of $Ce_{1-x}Zr_xO_2$ solution.

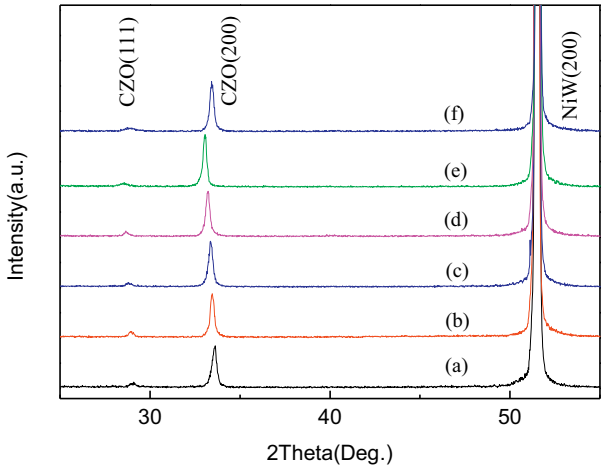


**Fig. 2.** XRD patterns of $\theta$–$2\theta$ scan for several buffer layers on NiW substrate, (a) NiW/$Ce_{0.75}Zr_{0.25}O_2$;(b) NiW/$Ce_{0.8}Zr_{0.2}O_2$;(c) NiW/$Ce_{0.85}Zr_{0.15}O_2$; (d) NiW/$Ce_{0.90}Zr_{0.1}O_2$;(e) NiW/$CeO_2$;(f) NiW/gradient CZO.

## 2. Experimental

CZO buffer layers were prepared through an inorganic-salts-based sol–gel route. The details for the synthesis of the precursor solution were shown in Fig. 1. Cerium nitrate ($Ce(NO_3)_3{\cdot}6H_2O$) and zirconium oxychloride ($ZrOCl_2{\cdot}8H_2O$) with stoichiometric proportions, as starting reagents, were dissolved in methanol under ambient conditions. After stirring continuously, a series of homogeneous $Ce_{1-x}Zr_xO_2$ sols with different Zr-doped concentration x of 0.25, 0.2, 0.15, 0.1 and 0.0 were obtained through adjusting the additive amount of cerium and zirconium in the precursor solutions. Textured NiW alloy tapes in this study were provided by Northwest Institute for Nonferrous Metal Research of China. Firstly, five kinds of monolayer films, named as $Ce_{0.75}Zr_{0.25}O_2$, $Ce_{0.8}Zr_{0.2}O_2$, $Ce_{0.85}Zr_{0.15}O_2$, $Ce_{0.9}Zr_{0.1}O_2$ and $CeO_2$, were prepared on the annealed NiW substrates (10 mm × 10 mm) by using a dip-coating technique. The variation of the lattice constant with the change of Zr-doped concentration x is investigated. And besides, a Zr-doped concentration gradient buffer architecture $Ce_{0.75}Zr_{0.25}O_2/Ce_{0.8}Zr_{0.2}O_2/Ce_{0.85}Zr_{0.15}O_2/Ce_{0.9}Zr_{0.1}O_2$ (called as $Ce_{1-x}Zr_xO_2$ (CZO) in what follows) was deposited under the same conditions. Each CZO film was dried at 80 °C for 10 min to remove the organic solvent, and further annealed at 1050 °C for 60 min under a flowing reducing mixed gas (96%Ar + 4%$H_2$).

The PLD system consisted of a standard PLD chamber and an excimer KrF laser ($\lambda$ = 248 nm) was used to prepare YBCO films on the gradient CZO buffer architecture. The pulsed laser energy density and the target-substrate distance were 1–1.8 J/$cm^2$ and 45 mm, respectively. The deposition temperature was controlled at 770 °C.

The structural properties and crystallinity of the samples were investigated by using an X-ray diffractometer (XRD, Shimadzu 7000S-type) operated with Cu Kα source. To evaluate the growth texture

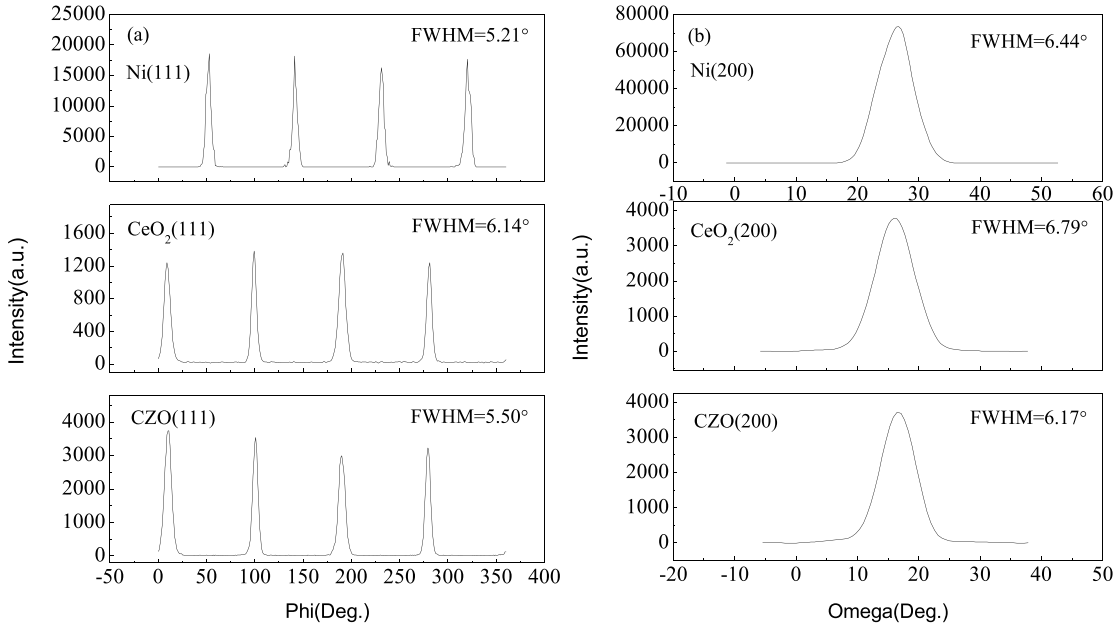


**Fig. 3.** Typical (111) phi-scans and (200) omega-scans of (a) NiW substrate, (b) pure $CeO_2$, and (c) gradient CZO.

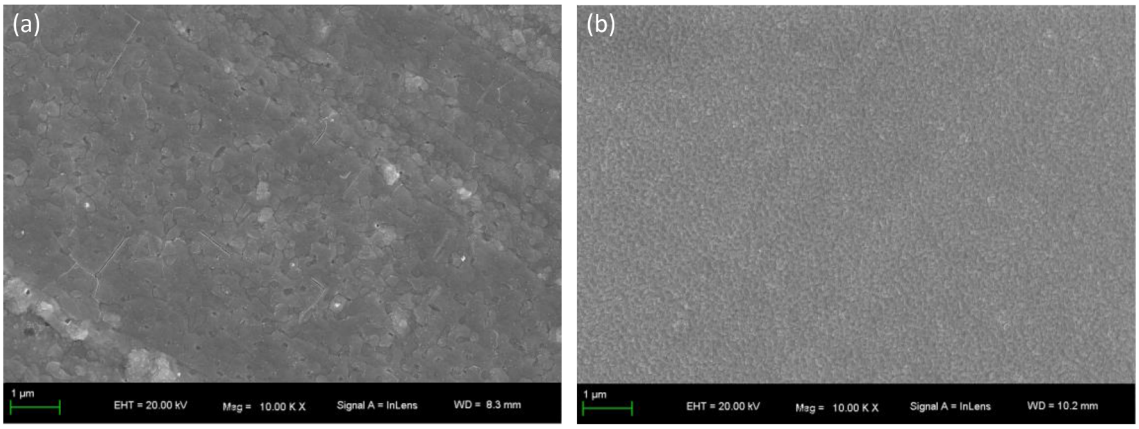


**Fig. 4.** SEM images of the buffer layer on biaxially textured NiW substrate. (a) pure $CeO_2$ buffer layer, (b) gradient CZO buffer layer.

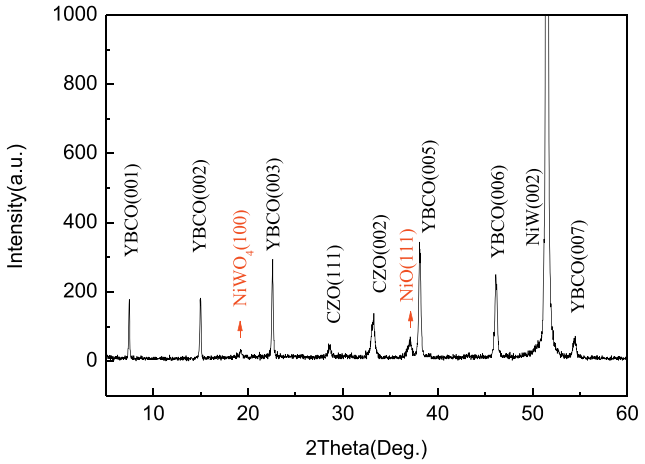


**Fig. 5.** XRD pattern of $\theta$–$2\theta$ scan for YBCO film epitaxially grown on gradient CZO buffered NiW substrate.

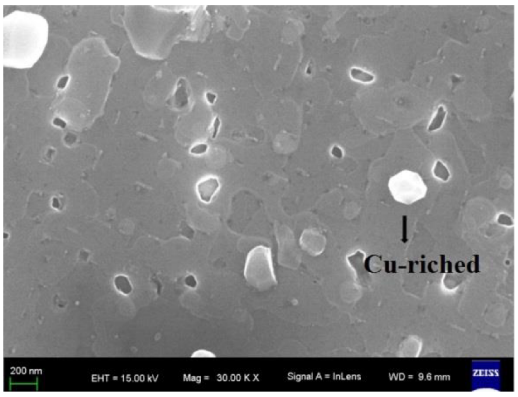


**Fig. 7.** SEM images of YBCO film epitaxially grown on gradient CZO buffered NiW substrate.

quality, the in-plane and out-of-plane textures of films were evaluated by a Rigaku SmartLab XRD with φ-scan and ω-scan (rocking curve) patterns. Scanning electron microscopy (SEM) experiments were conducted on a JEM-6700F to observe the surface morphologies. The cross-sectional morphology and the interface microstructure of NiW/CZO/YBCO multilayer were analyzed by a JEM-3010 high-resolution transmission electron microscope (HRTEM). Curves depicting the resistance-temperature ($R$–$T$) characteristics of the films were measured by a multi-function vibrating sample magnetometer (VersaLab). $J_c$ measurement was commissioned to the Northwestern Institute of Nonferrous Metals using a four-probe method.

## 3. Results and discussion

### 3.1. Epitaxial characteristics of buffer layer

X-ray diffraction $\theta$–$2\theta$ scans for several buffer layers are shown in Fig. 2. It can be seen that both the monolayer film and the gradient buffer layers exhibit good $c$-axis preferred orientation, as evidenced by strong (00l) peaks with negligible (111) peaks. The slight shift of the (002) peak can be attributed to a cell constant variation, which is

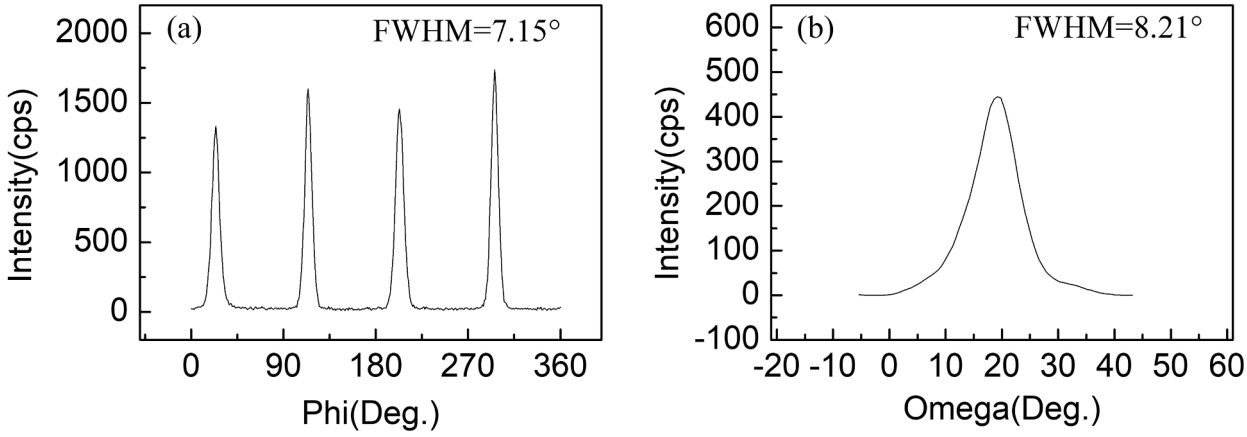


**Fig. 6.** XRD patterns of (a) $\varphi$-scan of (103) reflection, (b) $\omega$-scan of (005) reflection of YBCO film.

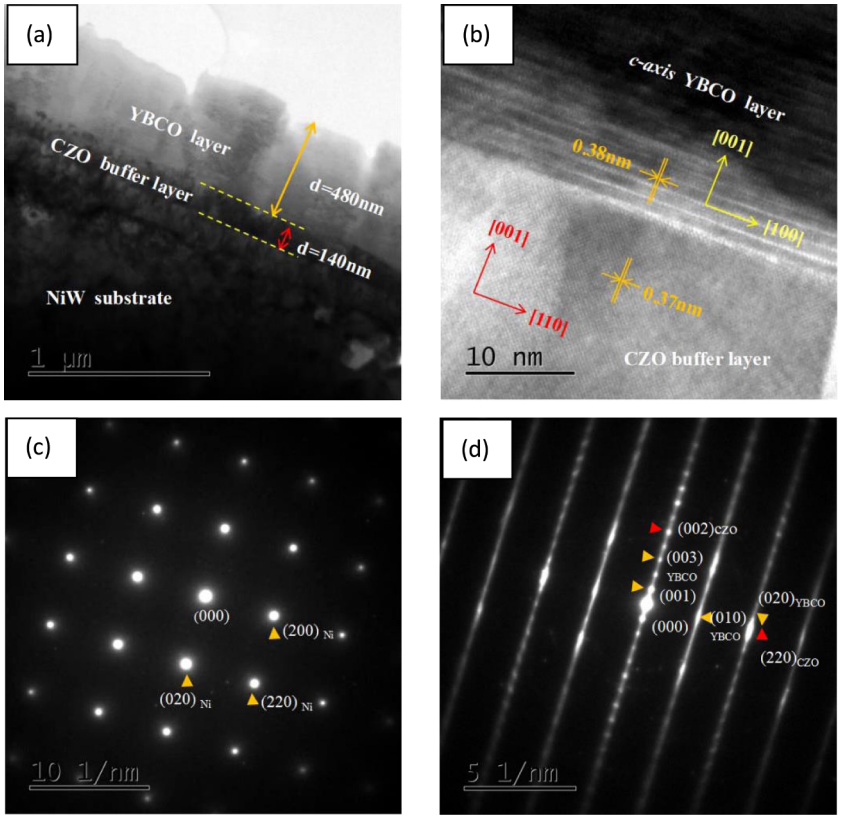


**Fig. 8.** Cross sectional TEM analysis of the NiW/CZO/YBCO sample. (a) Low-magnification TEM image of the whole sample, (b) high-magnification TEM image of CZO/YBCO interface, (c) SAED pattern of the cubic NiW, (d) SAED pattern of the cross section between YBCO and gradient CZO.

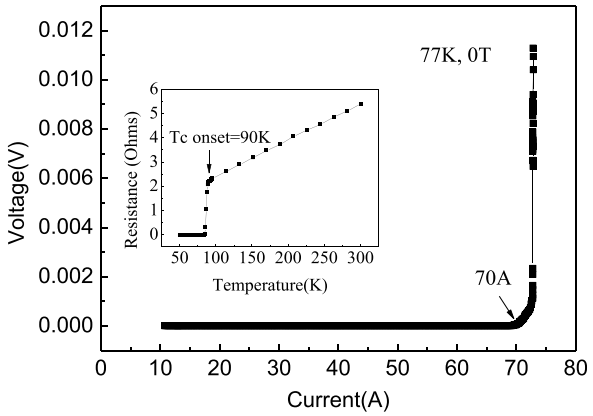


**Fig. 9.** *R–T* curve of YBCO film on gradient CZO buffered NiW substrate (Inset: V–I curve of this sample).

evaluated by the Bragg equation $2dsin\theta = n\lambda$. The lattice parameters of simple 2(a)–2(e) are 5.339 Å, 5.352 Å, 5.370 Å, 5.385 Å, 5.410 Å, respectively, demonstrating the lattice parameters also show a gradient variation with the change of Zr concentration, which is very close to theoretical values. As plotted in Fig. 2(f), the lattice parameter of gradient CZO buffer layer is 5.369 Å. It is noted that the calculated value is in the range of zirconium doping fraction x = 0.1 to x = 0.25. Besides, high diffraction peak intensity is presented in the gradient CZO buffer layer, indicating excellent structural matching characteristics between each layer. The above XRD results well support the feasibility that the gradient CZO can serve as good growth templates for YBCO superconducting films

To evaluate the quality of grain texture of buffer layer on NiW substrate, XRD φ-scan of (111) reflection and ω-scan of (200) reflection measurements are carried out and the results are presented in Fig. 3. The φ-scan of CZO films exhibit four-folder symmetric diffraction peaks and show an offset angle of 45° compared with the φ-scan of NiW substrate, indicating the epitaxial growth mode between substrate and buffer layer in a–b plane can be described as NiW[100]//CZO[110]. In a quantitative analysis, the gradient CZO shows sharper in plane and out plane crystallographic alignment, with the full width at half maximum (FWHM) values of 5.50°(Δφ) and 6.17°(Δω), as compared to 6.14°(Δφ) and 6.79°(Δω) for pure $CeO_2$. The specific interfacial characteristics, such as small lattice mismatch and interfacial stress between substrate and gradient CZO is probably the reasons of the better texture quality during the film nucleation under present conditions.

The surface morphology is confirmed by SEM, as shown in Fig. 4. The appearance of microcracks is normally associated with the release of residual stresses throughout pure $CeO_2$ buffer layer, caused by difference in thermal expansion and lattice parameters between the substrate and the $CeO_2$ material [17]. The element diffusion channels are easy to form in the crack area, which will weaken the barrier diffusion ability and cannot be used as a template for further epitaxial growth of superconducting layer. The gradient doping of zirconium is conducive to create relaxation spots [18], where a homogeneous, crack free and dense microstructure is discerned in the gradient CZO film. The laser scanning confocal microscope roughness measurement shows that the linear roughness (*Ra*) and surface roughness (*Sa*) values of pure $CeO_2$ are 0.034 μm and 0.004 μm, while the *Ra* and *Sa* values of gradient CZO are 0.007 μm and 0.001 μm, indicating zirconium doping has an obvious reduction effect of surface roughness of CZO buffer layer, which is favorable to increase the film thickness and reduce crack formation.

### 3.2. Microstructure and properties of coated conductors

The phase development of YBCO deposited on the gradient CZO buffer layer is characterized by means of x-ray diffraction. As shown in

Fig. 5, YBCO film exhibits *(00l)* preferred growth orientation (*c*-axis texture) and along with two small diffraction peaks at 19.2°($NiWO_4$) and 37.2°(NiO) which are corresponding to the common secondary phases in YBCO coated conductors. More details about the quantitative structural properties of YBCO film are confirmed by (103) phi scan and (005) rocking curve. It can be seen from Fig. 6, the FWHM values, which are representative of in-plane and out-of-plane textures, are 7.15° and 8.21°, respectively.

SEM surface morphology of the YBCO is shown in Fig. 7. The YBCO superconducting layers exhibit smooth morphology with a significant surface density, demonstrating the nanometer level flatness of the film grown on a buffer layer. The absence of a small amount of Cu-rich particles distribution is similar to those reported in other literature [19]. Generally, such island-like microstructural characteristics indicate pure *c*-axis orientation epitaxial growth of the YBCO film on the gradient CZO surface.

In order to investigate the micro-crystal structure and epitaxial relationship of YBCO film on NiW substrate, high resolution transmission electron microscopy (HRTEM) analysis is carried out and the results are presented in Fig. 8. It can be learned from Fig. 8(a) that the clear interface of CZO and YBCO are observed and the films thickness are calculated to be around 140 nm and 480 nm, respectively. The more clearly coherent interface is shown in Fig. 8(b). The YBCO film grows along *c*-axis, the (*00l*) direction, onto the gradient CZO buffer layer with clear lattice fringes and boundaries. The lattice fringe spacing of CZO intermediate layer and top YBCO layer are measured and the corresponding values are 0.37 nm, 0.38 nm, respectively, which are consistent with the interplanar spacing of CZO (110) plane and YBCO (100) plane. As shown in Fig. 8(c) and (d), the selected area electron diffraction(SAED) is conducted. The appearance of intensified diffraction spots in NiW reveals its cubic structure, where the crystal axis is [100]. A detailed analysis of SAED pattern in CZO/YBCO interface indicates the YBCO film is grown through a 45° in-plane rotation on the gradient CZO buffer layer with the relationship of CZO(220)//YBCO(020) as well as CZO(002)//YBCO(*00l*).

The temperature dependence of the normalized resistance (*R–T* curve) is obtained by the four-point contact technique and the result is shown in Fig. 9. The onset critical superconducting transition temperature ($T_c$) of the YBCO film is 90 K. The V–I curve of the sample is shown in the inset of Fig. 9. It exhibits a sharp transition from superconducting state to normal state when the current is above 70A/cm-w at 77 K self-field, and the calculated critical current density is around 1.9 MA/$cm^2$ (the thickness of the as-deposited YBCO film is estimated to be 480 nm according to TEM analysis). These values are comparable with the best of those reported by others [20,21]. The results show that gradient CZO can serve as a simplified buffer layer to transfer texture and block the diffusion of atoms.

## 4. Conclusions

The CZO buffer architecture with gradient change of Zr concentration along the thickness direction of film has been prepared on the biaxially textured NiW substrate, and then the YBCO film with an epitaxial relationship can subsequently grow on it. The conclusions are drawn out as follows:

(a) The gradient CZO prepared by sol–gel method shows a high *c*-axis texture. With the change of Zr concentration, the lattice parameters of each layer also show a gradient variation. The layer with a larger Zr concentration has a lattice parameter close to that of the NiW substrate, and the other layer with a lower Zr concentration is close to YBCO.

(b) Using Zr-doped concentration gradient architecture CZO as barrier layer to prepare NiW/CZO/YBCO coated conductor, The epitaxial growth relationship is NiW(002)//CZO(002)//YBCO(*00l*) and NiW (200)//CZO(220)//YBCO(020).

(c) YBCO film grown on the gradient CZO buffered NiW substrate exhibits good superconducting performance of $T_c$ (90 K) and $J_c$ (1.9 MA/$cm^2$), indicating that CZO can serve as a simplified buffer architecture to transfer texture and block the diffusion of atoms.

## Acknowledgments

This investigation is supported by the National Natural Science Foundation of China (nos. 51202190 and 51672212).

## References

[1] V. Mihalache, N. Stefan, I. Enculescu, et al., The influence of the microstructure and morphology of $CeO_2$ buffer layer on the properties of YBCO films PLD grown on Ni tape, J. Supercond. Novel Magn. 27 (11) (2014) 2475–2485.
[2] M. Colla, J. Gàxquez, R. Hühne, B. Holzapfel, Y. Morilla, J. García-López, A. Pomar, F. Sandiumenge, T. Puig, X. Obradorsb, All chemical $YBa_2Cu_3O_7$ superconducting multilayers: critical role of $CeO_2$ cap layer flatness, Mater. Res. Soc. 24 (4) (2009) 1446–1455.
[3] D. Xu, L. Liu, G. Xiao, Y. Wang, Y. Li, Improved textured $La_2Zr_2O_7$ buffer layers on bi-axially textured Ni–W substrates using $CeO_2$ seed layers for $YBa_2Cu_3O_{7-x}$ coated conductors, Thin Solid Films 548 (2013) 502–508.
[4] S. Engel, K. Knoth, R. Hühne, L. Schultz, B. Holzapfel, An all chemical solution deposition approach for the growth of highly textured $CeO_2$ cap layers on $La_2Zr_2O_7$-buffered long lengths of biaxially textured Ni–W substrates for YBCO-coated conductors, Supercond. Sci. Technol. 18 (2005) 1385.
[5] M.S. Bhuiyan, M. Paranthaman, S. Sathyamurthy, T. Aytug, S. Kang, D.F. Lee, A. Goyal, E.A. Payzant, K. Salama, MOD approach for the growth of epitaxial $CeO_2$ buffer layers on biaxially textured Ni-W substrates for YBCO coated conductors, Supercond. Sci. Technol. 16 (2003) 1305–1309.
[6] E. Bartolom´e, V.R. Vlad, A. Calleja, M. Aklalouch, R. Guzm´an, J. Arbiol, X. Granados, A. Palau, X. Obradors, T. Puig, A. Usoskin, Magnetic and structural characterization of inkjet-printed $^{TFA}YBa_2Cu_3O_{7-x}$/ $^{MOD}CZO$/$^{ABAD}YSZ$/SS coated conductors, Supercond. Sci. Technol. 26 (2013) 1250041–11.
[7] M.P. Siegal, P.G. Clem, J.T. Dawley, et al., Optimizing $SrTiO_3$ films on textured Ni substrates using chemical solution deposition, J. Mater. Res. 20 (4) (2005) 910–921.
[8] Y. Wang, H. Wang, C.S. Li, et al., Effective removal procedure of residual carbon in $CeO_{2-x}$, films fabricated via MOD method, Ceram. Int. 41 (10) (2015) 14270–14275.
[9] E.K. Athanassiou, P. Grossmann, R.N. Grass, et al., Comparative studies of nanostructural and morphological evolution of $CeO_2$ thinfilms, Nanotechnology (16) (2007) 165605–165613.
[10] P. Zhao, Z. Huang, Y. Mao, et al., Preparation of (100)-oriented $CeO_2$, film on (100) MgO single crystal substrate by laser chemical vapor deposition using solid precursor, Ceram. Int. 40 (10) (2014) 15919–15923.
[11] M. Paranthaman, A. Goyal, F.A. List, et al., Growth of biaxially textured buffer layers on rolled-Ni substrates by electron beam evaporation, Physica C 275 (3) (1997) 266–272.
[12] A. Al Ibrahim, A. Ilyushechkin, J. Rossiter, T. Yamashita, I.E. Agranovski, Application of spray deposition techniques for fabrication of Sm-doped $CeO_2$ thin films on biaxially textured Ni-W substrate, Surf. Coat. Technol. 272 (2015) 8–14.
[13] D.Q. Shi, J.H. Kim, M.Y. Zhu, S.X. Dou, $Ce_2Y_2O_7$ and $Ce_{0.8}Zr_{0.2}O_2$ buffer layers deposited by E-beam evaporation, Physica C 460–462 (2007) 1394.
[14] J. Xiong, B. Tao, W. Qin, X. Feng, X. Song, F. Zhang, Y. Li, Reel-to-reel continuous deposition of $Ce_xZr_{1-x}O_2$ single buffer layer for YBCO coated conductors, J. Phys. 153 (2009) 012036.
[15] J.M. Zeng, A. Ignatiev, Y.X. Zhou, K. Salama, A single oxide buffer layer on a cube-textured Ni substrate for the development of YBCO coated conductors by photo-assisted MOCVD, Supercond. Sci. Technol. 19 (2006) 772.
[16] V. Narayanan, S. Van Steenberge, P. Lommens, I. Van Driessche, Aqueous chemical solution deposition of novel, thick and dense lattice-matched single buffer layers suitable for YBCO coated conductors: preparation and characterization, Nanomaterials 2 (2012) 298–311.
[17] F. Sen, E. Celik, M. Toparli, Transient thermal stress analysis of CeO thin films on Ni substrates using finite element methods for YBCO coated conductor, Mater. Des. 28 (2) (2007) 708–712.
[18] M. Mogensen, N.M. Sammes, G.A. Tompsett, Physical, chemical and electrochemical properties of pure and doped ceria, Solid State Ionics 129 (1) (2000) 63–94.
[19] Y. Zhao, X.F. Li, A. Khoryushin, et al., Development of all chemical solution derived $Ce_{0.9}La_{0.1}O_{2-y}$/$Gd_2Zr_2O_7$ buffer layer stack for coated conductors: influence of the post-annealing process on surface crystallinity, Supercond. Sci. Technol. 25 (1) (2012) 24–24.
[20] P. Zhao, A. Ito, T. Goto, Orientation control and electrical properties of $YBa_2Cu_3O_{7-\delta}$, deposited onto $CeO_2$, buffer films by laser chemical vapor deposition using liquid source precursors, Thin Solid Films 564 (2014) 92–96.
[21] C. Ren, H.L. Suo, M. Liu, et al., Investigation on $La_2Zr_2O_7$ multilayers by chemical solution deposition, Ceram. Int. 43 (6) (2017).